Silicon Rice-Straw Array Emitters and Their Superior Electron Field Emission

Hung-Chi Wu,[†] Hung-Yin Tsai,[‡] Hsin-Tien Chiu,[||] and Chi-Young Lee*[,†,§]

Department of Materials Science and Engineering, Department of Power Mechanical Engineering, and Center for Nanotechnology, Materials Science, and Microsystems, National Tsing Hua University, Hsinchu 30013, Taiwan, Republic of China, and Department of Applied Chemistry, National Chiao Tung University, Hsinchu, Taiwan 30010, Republic of China

ABSTRACT Free standing and vertically aligned silicon rice-straw- like array emitters were fabricated by modified electroless metal deposition (EMD), using HF-H_2O_2 as an etching solution to reduce the emitter density and to make the emitter end of the formed silicon rice-straw arrays shaper than those formed by conventional EMD. These silicon rice-straw array emitters can be turned on at $E_0 = 4.7$ V/μm, yielding an EFE (electron field emission) current density of $J_e = 139\ \mu$A/cm^2 in an applied field of 12.8 V/μm. According to a simple simulation, the excellent EFE performance of the silicon rice-straw array emitters originates in not only the favorable distribution of emitter arrays, but also the shape of the emitter apexes. The modified-EMD method is easily scaled up without expensive equipment, so silicon rice-straw array emitters are a promising alternative to silicon-based field emitters.

KEYWORDS: one-dimensional • silicon • emitter • electroless metal deposition (EMD) • electron field emission (EFE) • simulation

INTRODUCTION

One-dimensional (1D) nanostructures, such as nanotubes, nanowires, and nanorods, have drawn much attention and have been widely explored as potential functional components in future electronic and optical systems (1, 2). Materials such as semiconductors (carbon, silicon, germanium) (3−5), metal oxides (zinc oxide, tungsten oxide, copper(I) oxide) (6−8), and metal silicides (titanium silicide, cobalt silicide, nickel silicide) (9−11) in nanostructures are regarded as ideal electric field emission (EFE) sources because of their high aspect ratio. Among these several 1D materials, silicon-based electric field emitters are the most interesting candidates for vacuum electronics devices, because silicon processing has already been extensively developed for very-large-scale integration (VLSI) fabrication, enabling atomically sharp silicon tips to be easily fabricated by isotropic or anisotropic etching.

Field emitter arrays have attracted considerable interest because their potential uses in high-frequency devices (12), flat panel displays (13), vacuum microelectronic devices (14), lithography (15), sensors (16), and microscopy (17). Various methods, including wet chemical etching (18), anodization (19), patterned reactive ion etching (RIE) combined with dry plasma etching (20), and chemical vapor deposition (CVD) (21), have been developed in recent decades to prepare silicon nanostructures that are used in field emitter arrays. Of these, anisotropic wet chemical etching, especially electroless metal deposition (EMD) using a mixed solution of hydrofluoric acid (HF) and silver nitrate ($AgNO_3$) has attracted substantial interest because it can be used relatively easy to fabricate well-aligned, single-crystalline, length-controllable, and wafer-scale arrays of silicon nanowire arrays at low temperatures (22).

However, in previous investigations, the strong screening effect of the crowded silicon wire arrays that are formed by EMD degrades the performance of electron field emission (23, 24). Because most of its applications require a high emission current and a low operating voltage, several approaches can be used to achieve these goals. They include sharpening the apex of the emitter tip to make it as small as possible, arranging the field emitters at the optimal distance from their neighbors, reducing the distance between the emitter and the gate electrode, and using materials with a low work function. In this study, typical crowded silicon wall-like arrays formed by conventional EMD are adapted by using modified etching to reduce the number of interconnected crowded arrays, yielding individually separated arrays with sharp apexes.

EXPERIMENTAL SECTION

A. Fabrication of Silicon Rice-Straw Array Emitters. Wall-like silicon arrays were obtained by a conventional-EMD method that involved immersing the cleaned [100]-oriented silicon wafer (As-doped, resistivity: 1−10 Ωcm) into 5.0 M HF and 20 mM $AgNO_3$ aqueous etching solution in a sealed vessel, and maintaining the system for 60 min at 323 K. The samples thus obtained were cleaned in HNO_3 and deionized water and then dried.

Silicon rice-straw arrays were prepared by dipping wall-like arrays in a mixed solution of 4.6 M HF and 10 mM $AgNO_3$ for 5 s to precipitate silver (Ag) particles as electrodes. They were then immersed at 323 K in 4.6 M HF and 23 mM H_2O_2 alcoholic

* Corresponding author. E-mail: cylee@mx.nthu.edu.tw.
Received for review August 9, 2010 and accepted October 7, 2010
[†] Department of Materials Science and Engineering, National Tsing Hua University.
[‡] Department of Power Mechanical Engineering, National Tsing Hua University.
[§] Center for Nanotechnology, Materials Science, and Microsystems, National Tsing Hua University.
[||] National Chiao Tung University.
DOI: 10.1021/am100716y

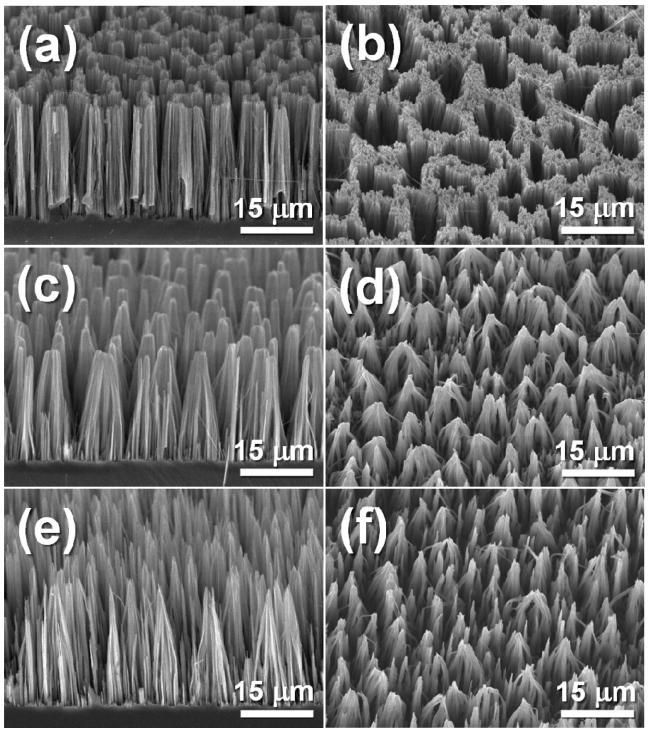

FIGURE 1. Cross-sectional and tilt-view SEM images of (a, b) EMD-Si, which was fabricated by conventional EMD; (c, d) SiA−1, and (e, f) SiA−2, which were reformed from EMD-Si by applying modified-EMD once and twice, respectively.

solution to induce an electrochemical redox reaction for 10 min. They were cleaned in nitric acid and deionized water and then dried.

B. Characterization. The surface morphologies of the as-synthesized samples were determined by scanning electron microscopy (SEM, JEOL 6500F). EFE measurements were made in a system that was built for this purpose in the laboratory at a base pressure of 3×10^{-6} Pa. The sample was fixed on a stainless steel holder and used as a cathode. The anode was a rod-like molybdenum probe with a diameter in 1 mm. The distance from the anode to sample was around 50 μm. A direct current voltage that was swept from 0 to 1100 V in steps of 20 V was applied to the sample. The dependence of the field emission current on the potential difference between the anode and the cathode (IV behavior) was recorded automatically using a Keithley 2410 source meter at intervals of 1 s.

RESULTS AND DISCUSSION

Images a and b in Figure 1 present SEM images of conventional EMD treated silicon wafers, which were designed as **EMD-Si**. The top-view of EMD-Si shows irregular shaped pores with porous wall. The side-view of EMD-Si appears as mountains whose summits were removed by an excavator. This special morphology was formed by a Galvanic etching process that was facilitated by Ag particles, as described elsewhere (22). The most preferred direction of etching of the silicon wafer was [100] (25), which resulted in the formation of vertically aligned [100]-oriented wall-like silicon arrays on a [100] silicon wafer. Although EMD was a simple method for fabricating [100]-oriented silicon arrays, the EFE properties of these arrays were not as favorable as expected. The obstacle to the use of these wall-like arrays as an EFE emitter is that they contain crowded and joined large sized lumps.

Table 1. Electron Field Emission Properties of Silicon Array Emitters in This Study

	EMD-Si	SiA−1	SiA−2
E_0 (V/μm)	13.8−14.3	8.9−9.1	4.7−4.8
J_e (μm/cm^2) at E_a (V/μm)	~34 (24.5)	~91 (22.7)	~139 (12.8)
β	~561	~887	~1406

To improve the EFE properties, EMD-Si was sharpened using a modified-EMD process. First, Ag particles were formed on the tips and upper side wall of the EMD-Si by dipping it in the $AgNO_3$ solution. Further etching was then performed in HF-H_2O_2 solution in alcohol. Images c and d in Figure 1 and images e and f in Figure 1 present SEM images of samples that were obtained by treating EMD-Si once and twice by the modified-EMD process to form silicon array−1 (SiA−1) and silicon array−2 (SiA−2). Unlike EMD−Si, SiA−1 and SiA−2 comprise thick and thin bunches of rice-straw-like silicon wire arrays, respectively. After they were immersed in the modified-EMD solution, the joined lumps were separated by etching the contacts between lumps (the distribution densities of EMD-Si and SiA−1 were shown in Supporting Information, Figure S1). Because SiA−2 was obtained further etching of SiA−1, bunches may be sharpened and divided into thin bunches, therefore, the number density of silicon wire bunches in SiA−2 could be larger than that of SiA−1. The sizes of the tips of the SiA−1 and SiA−2 bunches were around 0.5−4 and 0.3−2.5 μm, respectively. The individual free-standing silicon wire bunch arrays with sharp apexes are expected to exhibit a superior EFE property.

Table 1 summarizes the EFE properties of EMD-Si, SiA−1, and SiA−2 (as described by the Supporting Information). Moreover, Figure 2a presents the current density-applied electric field (J-E) plot and Figure 2b shows the corresponding Fowler−Nordheim (F−N) plot of the field emission properties of these silicon arrays as emitters. Crowded wall-like arrays in EMD-Si vertically aligned on the silicon substrate require a large turn-on field, $(E_0)_{EMD\text{-}Si} = 14.0$ V/μm, to induce EFE and can reach a current density $(J_e)_{EMD\text{-}Si} = 34$ μA/cm^2 in an applied field of $(E_a)_{EMD\text{-}Si} = 24.5$ V/μm. SiA−1 had been improved by reduced emission densities and sharpened tips, yielding a turn-on field of $(E_0)_{SiA-1} = 8.9$ V/μm and a current

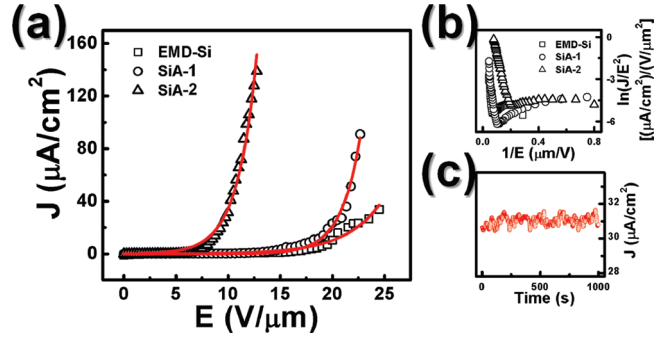

FIGURE 2. (a) Field emission current density from silicon emitter arrays against applied electric field: EMD-Si (square), SiA−1 (circle), and SiA−2 (triangle); (b) corresponding F−N plot, which reveals linear dependence and the consistency between the emission and the F−N mechanism; (c) stability test of SiA−2 under 10 V/μm for 1000 s.

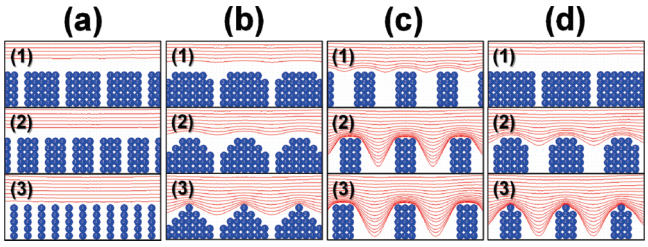

FIGURE 3. Simulation of penetration of equipotential lines in an identical electrostatic field for emitters with various (a) aspect ratios, (b) tip geometries, and (c) interdistances between the emitters; (d) assumed model.

density of $(J_e)_{SiA-1} = 91\ \mu A/cm^2$ in an applied field of $(E_a)_{SiA-1} = 22.7\ V/\mu m$. The turn-on field of SiA−2 was $(E_0)_{SiA-2} = 4.7\ V/\mu m$, and a current density of $(J_e)_{SiA-2} = 139\ \mu A/cm^2$ was reached in an applied field of $(E_a)_{SiA-2} = 12.8\ V/\mu m$. The field enhancement factor (β) of each specimen is estimated using the F−N equation, yielding $(\beta)_{EMD\text{-}Si} = 561$, $(\beta)_{SiA-1} = 887$ and $(\beta)_{SiA-2} = 1406$ for the three silicon array emitters, respectively. In addition, the EFE stability of SiA−2 was examined by measuring the current density at the constant electric field, 10 V/μm, as shown in Figure 2c. The current density fluctuation was less than 2 $\mu A/cm^2$ during the measurement period.

The EFE properties of SiA−2 obtained via a simple wet etching process are as good as those of other silicon array emitters that were fabricated by different procedures, such as chemical vapor deposition (26, 27), annealing method (28), and lithography coupled with reactive ion etching (29, 30). Although highly ordered triangular silicon nanopillars with sharp tips fabricated by reactive ion etching accompanied nanosphere lithography on patterned silicon substrate have a relatively lower turn-on field around 1.6 V/μm (30). The simple, cheap, and easily scaled-up fabrication method make SiA−2 the most promising candidate for using in electron emitter applications. The turn-on fields and synthesized methods of the silicon emitters were shown in the Supporting Information (Table S1).

As is well-known, the shape and distribution of an emitter greatly affects its EFE properties in a manner that is indicated by an field enhancement factor, β, which is itself considered to be physically influenced by an internal factor "β_{in}" (tip morphology) and external factor "β_{ext}" (distribution) (31, 32). As an emitter has either a high aspect ratio or a sharp tip, the value of β_{in} is large; while the emitters are crowded, the value of β_{ext} is small. To confirm the observations in this investigation, we calculated the penetrations of the fields into the parallel standing emitters to be of similar heights but different shapes and distributions under an identical parallel electrostatic field (33) by using an electric field simulator (34), as shown in Figure 3. Based on the calculations, the electrostatic equipotential gradient near the emitters increased as the aspect ratio increased and as the diameter of the tip decreased. As the interval between the emitters increased, the gradient of equipotential near the emitters increased greatly until the interemitter distance was one to two times the height of the emitter (Figure 3c−2), at which it remained constant as the distance between the emitters increased further (Figure 3c−3). This result agrees with the theoretical studies of EFE properties for CNTs (33).

Figure 3d presents the assumed models of emission from EMD-Si, SiA−1, and SiA−2 which are: bulk emitters, individual separated thick arrays and individual separated thin arrays, respectively. EMD-Si arrays with bunched wires are assumed to have small β_{in} and β_{ext} values and thus require a strong external electric field to induce the emission of electrons. Since the interconnected bunched arrays were etched by a modified-EMD process to form individually separated arrays, SiA−1, and so the β_{ext} value increased as expected. Further etching sharpened the tip of the silicon arrays, increasing β_{in}. Therefore, we suggest that the EFE properties of SiA−1 were improved mainly by the increase in the interemitter distance and the reduction of the size of the tip, increasing both β_{ext} and β_{in}. The EFE properties of SiA−2 were improved further by the sharpening of tip, increasing only β_{in}.

CONCLUSION

Sharpened rice-straw like silicon emitter array (SiA−2) that stand vertically perpendicular to the substrate were reformed from wall-like silicon arrays (EMD-Si) by applying the modified-EMD method twice. The number of silicon emitter arrays was significantly lower than that of EMD-Si. SiA−2 has excellent EFE properties with a low turn-on field of 4.7 V/μm, a higher β value, and a higher current density than the crowded EMD-Si. On the basis of a simulation and experimental results, the improvement in the EFE performance from crowded EMD-Si to SiA−1 arises in the geometry of the separated individual emitter arrays and the sharper apexes of the emitter tips. The enhancement of EFE properties from SiA−1 to SiA−2 was mainly associated with sharpening of the tip. The fabrication of SiA−2 with sharp tips by reforming EMD-Si using the modified-EMD approach is an electroless self-alignment process without prepatterning. The fabrication of SiA−2 is much simpler, less expensive, and more easily scalable than that of silicon emitter arrays with sharp tips. Given all of these benefits, SiA−2 is recommended for use in electron emitter applications.

Acknowledgment. The authors would like to thank the National Science Council of the Republic of China, Taiwan, for financially supporting this research under Contract NSC-96-2113-M-007-021.

Supporting Information Available: Figure S1, estimation pixels of SEM images of EMD-Si and SiA−1; EFE parameters determination; Table S1, comparison of EFE properties between silicon emitter arrays obtained via various synthesized method (PDF). This material is available free of charge via the Internet at http://pubs.acs.org.

REFERENCES AND NOTES

(1) Yang, P. D.; Yan, R. X.; Fardy, M. *Nano Lett.* **2010**, *10*, 1529–1536.
(2) Chen, L. J. *J. Mater. Chem.* **2007**, *17*, 4639–4643.
(3) DeHeer, W. A.; Chatelain, A.; Ugarte, D. *Science* **1995**, *270*, 1179–1180.
(4) Huang, G. S.; Wu, X. L.; Cheng, Y. C.; Li, X. F.; Luo, S. H.; Feng, T.; Chu, P. K. *Nanotechnology* **2006**, *17*, 5573–5576.

(5) Li, L.; Fang, X. S.; Chew, H. G.; Zheng, F.; Liew, T. H.; Xu, X. J.; Zhang, Y. X.; Pan, S. S.; Li, G. H.; Zhang, L. D. *Adv. Funct. Mater.* **2008**, *18*, 1080–1088.
(6) Zhang, Z.; Meng, G. W.; Xu, Q. L.; Hu, Y. M.; Wu, Q.; Hu, Z. *J. Phys. Chem. C* **2010**, *114*, 189–193.
(7) Chang, M. T.; Chou, L. J.; Chueh, Y. L.; Lee, Y. C.; Hsieh, C. H.; Chen, C. D.; Lan, Y. W.; Chen, L. J. *Small* **2007**, *3*, 658–664.
(8) Hsieh, C. T.; Chen, J. M.; Lin, H. H.; Shih, H. C. *Appl. Phys. Lett.* **2003**, *83*, 3383–3385.
(9) Lin, H. K.; Tzeng, Y. F.; Wang, C. H.; Tai, N. H.; Lin, I. N.; Lee, C. Y.; Chiu, H. T. *Chem. Mater.* **2008**, *20*, 2429–2431.
(10) Tsai, C. I.; Yeh, P. H.; Wang, C. Y.; Wu, H. W.; Chen, U. S.; Lu, M. Y.; Wu, W. W.; Chen, L. J.; Wang, Z. L. *Cryst. Growth Des.* **2009**, *9*, 4514–4518.
(11) Lee, C. Y.; Lu, M. P.; Liao, K. F.; Lee, W. F.; Huang, C. T.; Chen, S. Y.; Chen, L. J. *J. Phys. Chem. C* **2009**, *113*, 2286–2289.
(12) Jensen, K. L.; Abrams, R. H.; Parker, R. K. *J. Vac. Sci. Technol. B* **1998**, *16*, 749–753.
(13) Spindt, C. A.; Holland, C. E.; Brodie, I.; Mooney, J. B.; Westerberg, E. R. *IEEE Trans. Electron Dev.* **1989**, *36*, 225–228.
(14) Lin, M. C.; Huang, K. H.; Lu, P. S.; Lin, P. Y.; Jao, R. F. *J. Vac. Sci. Technol. B* **2005**, *23*, 849–852.
(15) Kojima, A.; Ohyi, H.; Koshida, N. *J. Vac. Sci. Technol. B* **2008**, *26*, 2064–2068.
(16) Lee, K.; Holbert, K. E. *J. Electrochem. Soc.* **2004**, *151*, H81–H85.
(17) Honjo, I.; Endo, Y.; Goto, S. *J. Vac. Sci. Technol. B* **1997**, *15*, 2741–2748.
(18) Love, J. C.; Paul, K. E.; Whitesides, G. M. *Adv. Mater.* **2001**, *13*, 604–607.
(19) Kuan, C. Y.; Chou, J. M.; Leu, I. C.; Hon, M. H. *Electrochem. Commun.* **2007**, *9*, 2093–2097.
(20) Seeger, K.; Palmer, R. E. *Appl. Phys. Lett.* **1999**, *74*, 1627–1629.
(21) Lee, Y. D.; Lee, H. J.; Han, J. H.; Yoo, J. E.; Lee, Y. H.; Kirn, J. K.; Nahm, S.; Ju, B. K. *J. Phys. Chem. B* **2006**, *110*, 5310–5314.
(22) Peng, K. Q.; Wu, Y.; Fang, H.; Zhong, X. Y.; Xu, Y.; Zhu, J. *Angew. Chem., Int. Ed.* **2005**, *44*, 2737–2742.
(23) Tzeng, Y. F.; Wu, H. C.; Sheng, P. S.; Tai, N. H.; Chiu, H. T.; Lee, C. Y.; Lin, I. N. *ACS Appl. Mater. Interface* **2010**, *2*, 331–334.
(24) Wu, H. C.; Tsai, T. Y.; Chu, F. H.; Tai, N. H.; Lin, H. N.; Chiu, H. T.; Lee, C. Y. *J. Phys. Chem. C* **2010**, *114*, 130–133.
(25) Chen, C. Y.; Wu, C. S.; Chou, C. J.; Yen, T. J. *Adv. Mater.* **2008**, *20*, 3811–3815.
(26) Huang, C. T.; Hsin, C. L.; Huang, K. W.; Lee, C. Y.; Yeh, P. H.; Chen, U. S.; Chen, L. J. *Appl. Phys. Lett.* **2007**, *91*, 093133.
(27) Riccitelli, R.; Di; Carlo, A.; Fiori, A.; Orlanducci, S.; Terranova, M. L.; Santoni, A.; Fantoni, R.; Rufoloni, A.; Villacorta, F. J. *J. Appl. Phys.* **2007**, *102*, 054906.
(28) Chueh, Y. L.; Chou, L. J.; Cheng, S. L.; He, J. H.; Wu, W. W.; Chen, L. J. *Appl. Phys. Lett.* **2005**, *86*, 133112.
(29) Li, W.; Zhou, J.; Zhang, X. G.; Xu, J.; Xu, L.; Zhao, W. M.; Sun, P.; Song, F. Q.; Wan, J. G.; Chen, K. J. *Nanotechnology* **2008**, *19*, 135308.
(30) Hsieh, H. Y.; Huang, S. H.; Liao, K. F.; Su, S. K.; Lai, C. H.; Chen, L. J. *Nanotechnology* **2007**, *18*, 505305.
(31) Li, C.; Di, Y. S.; Lei, W.; Yin, Q.; Zhang, X. B.; Zhao, Z. W. *J. Phys. Chem. C* **2008**, *112*, 13447–13449.
(32) Spindt, C. A.; Brodie, I.; Hunphrey, L.; Westerberg, E. R. *J. Appl. Phys.* **1976**, *47*, 5248–5263.
(33) Nilsson, L.; Groening, O.; Emmenegger, C.; Kuettel, O.; Schaller, E.; Schlapbach, L.; Kind, H.; Bonard, J. M.; Kern, K. *Appl. Phys. Lett.* **2000**, *76*, 2071–2073.
(34) The free simulator is "Electric Field", and it can be obtained at the website: http://www.physics-software.com/software.html.

AM100716Y